Indian Journal of Chemical Technology
Vol. 17, May 2010, pp. 191-197

Photocatalytic activity of TiO_2:$AlPO_4$-5 zeolites for the degradation of Indigo caramine dye

B V Suresh Kumar*, C P Sajan, K M Lokanatha Rai[1] & K Byrappa

*Department of Studies in Geology, [1]Department of Studies in Chemistry, University of Mysore, Manasagangotri, Mysore 570 006, India
Email: bvsureshkumar@yahoo.com

Received 8 June 2009; revised 24 March 2010

Aluminophosphate zeolite ($AlPO_4$-5) coated or impregnated by clusters of TiO_2 were prepared under hydrothermal conditions (Temperature, ~150°C; Pressure is autogenous). These composite materials were subjected to a systematic characterization using X-ray diffraction, Fourier transform infrared spectroscopy, Scanning electron microscopy and BET surface area measurements. The encapsulation of TiO_2 in the $AlPO_4$ zeolite framework was confirmed by the profile analysis of X-ray diffraction patterns. The resultant products were employed successfully in the degradation of Indigo carmine dye. The effect of pH and the efficiency of composite materials on the degradation of Indigo carmine dye have been worked out. The decrease in the chemical oxygen demand proved the decomposition of harmful organics present in the dye solution.

Keywords*:* Aluminophosphate composites, Catalytic properties, Indigo caramine dye, Degradation

Heterogeneous photocatalysis has been widely accepted as a promising method for the treatment of trace organic pollutants both in water and air. Due to its unique feature of the complete mineralization of pollutants, without causing secondary pollution, heterogeneous photocatalysis has been extensively studied[1]. TiO_2 photocatalysts have been applied to environmental applications, such as for the treatment of air and wastewaters and as deodorizers, because of their strong oxidizing power, high photocatalytic activity, self-cleaning function, and bactericidal and detoxification activities[2-5]. Zeolites possess large surface areas, internal pore volume, unique uniform pores, and channel size[6-12], which are interesting hosts to disperse semiconductor photocatalyst on their surfaces. Surface areas in the range of 400-650 $m^2\ g^{-1}$ with pore volumes of above 0.1 $cm^3\ g^{-1}$ are common for conventional zeolites. Zeolites exhibit several other specific features[8,13,14] that make them suitable for their use as hosts for photocatalysts. The aluminophosphate zeolites ($AlPO_4$-5) coated or impregnated clusters of TiO_2 act as efficient photocatalysts for the decomposition of NO into N_2 and O_2, efficient removal of ammonia and hydrogen sulphide from air and the reduction of CO_2 with H_2O. Also in the liquid phase, this $AlPO_4$-5 zeolite containing titanium can affect the degradation of organic materials in wastewater[8]. It is well known that the aluminophosphate molecular sieves zeolites ($AlPO_4$-5) are highly crystalline and absorbed materials do not affect the crystal structure[8,10,11]. TiO_2 is known as photocatalytic material capable of decomposing a large variety of toxic and hazardous industrial effluents, upon exposure to either sun light or UV light under ambient temperature[15]. Upon photoexcitation, an encapsulated TiO_2 molecule can eject an electron, which will delocalize through the zeolite framework structure or in clusters of charge balancing cations. Also, there are reverse processes in which electron rich sites of the zeolites can donate an electron to a photo excited molecule. The method of encapsulation of TiO_2 in zeolite framework, without losing the photosensitization of TiO_2 and the adsorption properties of $AlPO_4$ zeolites is an important aspect while preparing zeolite based photocatalyst[16,17]. In the present work, authors report coating or impregnation of TiO_2 molecules in the framework of $AlPO_4$-5 zeolites and their application in photo degradation of Indigo caramine dye.

Experimental Procedure

Preparation of TiO_2:$AlPO_4$-5 zeolite

In the present work, the microporous aluminophosphate zeolites ($AlPO_4$-5) have been crystallized using hydrothermal method. Fig. 1 shows

the flow chart of $AlPO_4$-5 zeolite synthesis. The experimental conditions used in the crystallization process were:

(i) Neutralization of the pseudobohemite (AlOOH) suspended in water with equimolar amount of dilute orthophosphoric acid (H_3PO_4) to obtain the reactive aluminophosphate gel, (ii) Aging of the reactive aluminophosphate gel, (iii) Addition of organic amines to the reactive aluminophosphate gel. This is referred to as precursor gel, (iv) Aging of the precursor gel and finally (v) Closed hydrothermal treatment of the precursor gel.

The experimental run was carried out in PTFE (poly tetra fluoro ethylene) Teflon lined autoclaves made of SS316. The time duration for crystallization is 24 h at 150°C. After the experimental run, the autoclaves were quenched initially using an air jet and then with water, and the products were washed thoroughly using double distilled water and ultrasonicated to remove all the excess organic templates. A known amount of L.R grade TiO_2 was taken with 1 mol HCl and mixed thoroughly. This mixture is transferred to 30 mL Teflon lined autoclaves. The percent fill was maintained to 40%. Experimental run was carried out at 150°C for 24 h in hot air oven. Autoclaves were quenched using an air jet and then water. The run products were recovered carefully using double distilled water and dried at 50°C in a dust proof environment. The obtained TiO_2 is grained thoroughly with $AlPO_4$-5 with sufficient water. This mixture is treated hydrothermally at 150°C for 24 h. The resultant run product TiO_2:$AlPO_4$-5 was carefully recovered using double distilled water and dried at 50°C in a dust proof environment.

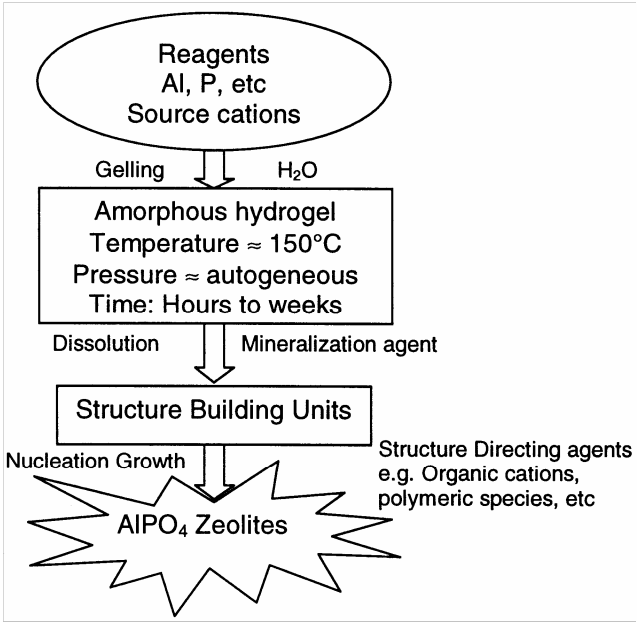

Fig. 1— Schematic diagram of $AlPO_4$-5 zeolite synthesis

Analysis

The materials obtained were subjected to powder X-ray diffraction, FTIR and SEM analysis. The X-ray diffraction patterns were recorded using Bruker AXS (Germany) Model: D8 (Advance). The X-rays used were CuKα with λ=1.5404 Å. The samples were scanned from 10° to 60°. FTIR spectra were recorded in the range of 400 to 4000 cm^{-1}, using FTIR spectrophotometer, JASCO-460 Plus, Japan and scanning electron micrographs (SEM) were recorded using a high resolution scanning electron microscopy, Hitachi, Model S-4000, Japan. The BET surface area measurements of the TiO_2:$AlPO_4$-5 zeolites were carried out using Shimadzu Flowsorb II Model No. 2305, Japan.

Results and Discussion

X- ray diffraction

Powder X-ray diffraction patterns showing 2 theta, intensity and *hkl* values of TiO_2:$AlPO_4$-5 and for the $AlPO_4$-5 are presented in Fig. 2. The XRD data were compared with the JCPDS files 500054, 211272 respectively. It is interesting to note the effect of the incorporation of TiO_2 ions in $AlPO_4$ zeolites, resulting in the significant decrease in the cell volume. The grain size of TiO_2:$AlPO_4$-5, $AlPO_4$-5 and TiO_2 are 55.249, 48.864, 6.385 nm respectively carried out by

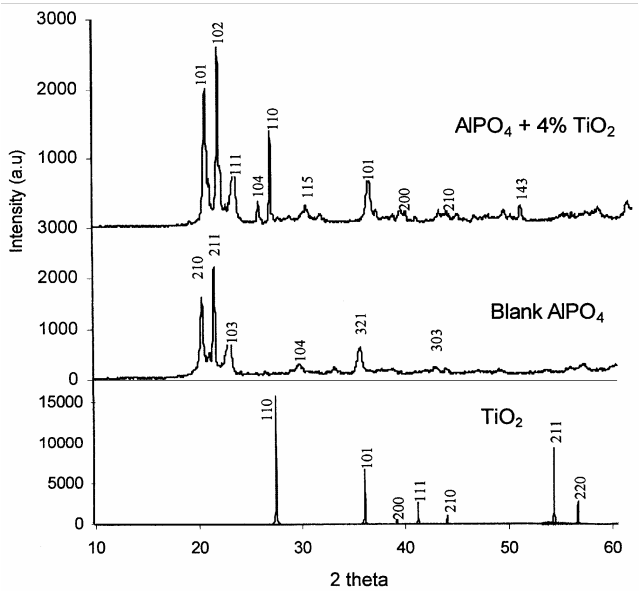

Fig. 2— XRD patterns of $AlPO_4$-5 and TiO_2:$AlPO_4$-5 composites

profile analysis of XRD pattern. In the region 2 theta 26.5 represents the presence of TiO_2 particles. This clearly proves that the TiO_2 particles are coated and impregnated in the cages of ($AlPO_4$-5) zeolites.

Infrared spectroscopy

The infrared spectra were recorded for $AlPO_4$-5, TiO_2 and TiO_2:$AlPO_4$-5 independently. Figure 3 shows the comparison of spectra of the samples. From the FTIR spectra the following observations are made. The sharp peak around 1100-1350 cm^{-1} is an exclusive feature of ($AlPO_4$-5) zeolites that contains the hydrated triple crankshaft chains. The strongest vibration in this region is assigned to a P-O stretch involving motions primarily associated with oxygen atoms or alternatively described as an asymmetric stretching mode[18] ← O P →← O. After the incorporation of TiO_2 into the $AlPO_4$-5 pores the band at this region is intensified. The P=O frequency is sensitive to the substitution. The broad band around 1100 cm^{-1} has been assigned to the asymmetric stretching of PO_4 tetrahedra[19]. The absorption peaks at 700 to 750 cm^{-1} correspond to the symmetric stretching vibration of PO_4 groups. The symmetric TO_4 stretching region in the spectra and sharp medium bands around 541 and 472 cm^{-1} are observed. These absorptions are either due to TO_4 bending or the motion of the external linkage of the AlO_4 and PO_4 tetrahedra. The weak band at 1398-1471 cm^{-1} may be affected by the non-structural alumina present in the pores. The broad weak band around 3000 to 3700 cm^{-1} is attributed to the stretching vibration of hydrogen group of water molecules and amines present in the pores of the $AlPO_4$-5 zeolites.

Scanning Electron Microscopy

The morphology and size of the ($AlPO_4$-5) and TiO_2: ($AlPO_4$-5) composites are shown in the Fig. 4. It is evident from the SEM photographs that the particle size has increased after the incorporation of TiO_2 into the pores of ($AlPO_4$-5). The surface morphology also changed from smooth, layered to rugged.

BET surface area measurements

BET surface area measurements were carried out for TiO_2:$AlPO_4$-5 zeolites to measure the total surface area of porous materials. About 0.5 g of the respective sample was degassed for 1 h at 250°C, using high purity nitrogen and helium gases in 80:20 ratios. Then the sample tube was fixed to the analyzer along with the balance tube and was kept in the nitrogen bath. The sample and balance tubes were evacuated initially followed by the nitrogen gas purging for the

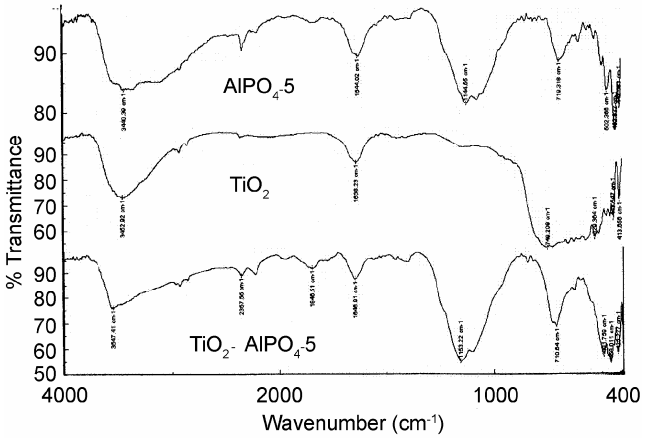

Fig. 3— FTIR patterns of ($AlPO_4$-5), TiO_2 and TiO_2:($AlPO_4$-5) composites

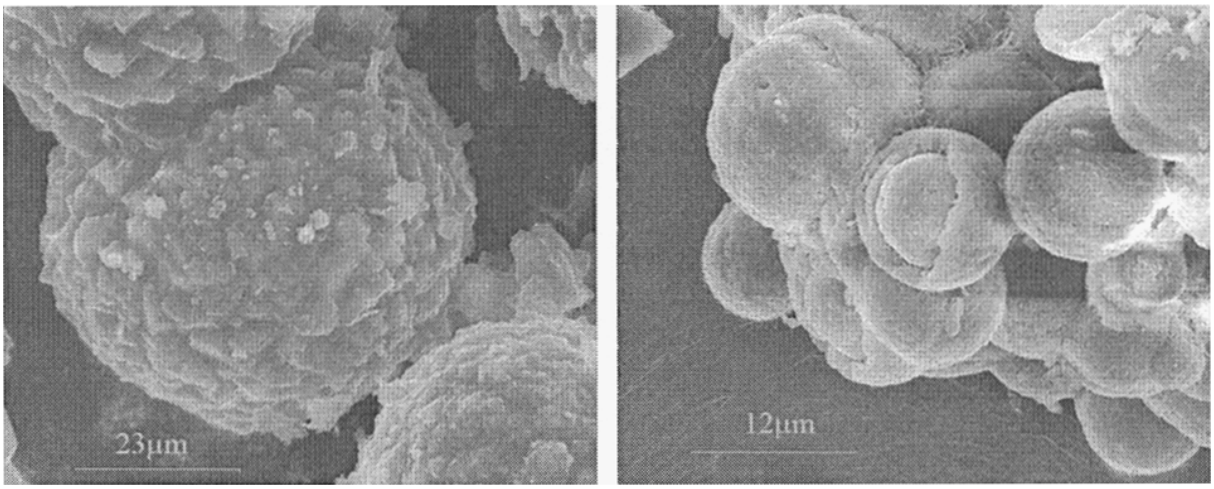

Fig. 4— Scanning electron micrographs of (a) ($AlPO_4$-5), and (b) TiO_2:($AlPO_4$-5) composites

adsorption. The average specific surface area from the six absorption cycles for each sample was calculated using Micrometric software. It is very clear that the average specific surface area of the $AlPO_4$-5 zeolites (54.05 m^2 g^{-1}) is strongly dependent on the percentage weight of TiO_2. The decrease in the surface area of TiO_2: $AlPO_4$-5 (9.12 m^2 g^{-1}) is because of the entry of TiO_2 particles into the pores and channels and blocking the same.

Photocatalytic activity of TiO_2:$AlPO_4$-5 composites

In the photocatalytic treatment of indigo carmine dye of a known concentration of 1 x 10^{-5} M dye solution (50 mL) was taken in a 500 mL clean beaker. To this dye solution a known amount of catalyst TiO_2: ($AlPO_4$-5) was added. It should be noted that no external supply of oxygen was employed. Then the beaker was exposed to the sunlight or UV light. The intensity of UV and sunlight was estimated by photolysis of uranil oxalate[20]. The intensity of UV was estimated as 2.3775 x 10^{15} quanta per second and the intensity of sunlight was estimated as 6.722 x 10^{16} quanta per second. Chemical oxygen demand (COD) was estimated before and after the treatment (using $K_2Cr_2O_7$ oxidation method) for the photocatalytic experiment in the present work.

The efficiency of the semiconductor used in the photocatalytic reaction depends on various parameters such as nature and concentration of the organic substrate, concentration and type of semiconductor, nature of the light source and its intensity, pH of the medium[21-24]. Figure 5 illustrates the comparative study of the effect of TiO_2:$AlPO_4$-5 and TiO_2 on percent transmission (%T) of indigo caramine dye under UV light as well as sun light.

Effect of pH

The pH of an aqueous dye solution affects all oxide semiconductors, including the surface charge on the semiconductor designer particulates, the size of the aggregates formed and the energies of conductance and valence band[25]. It is reported that both the acidic and basic media influence the efficiency of photodegadation reaction[19]. Figure 6 shows the effect of the pH versus percent transmission (%T). In the present work the pH of the dye solution was adjusted using varying concentration of HNO_3 and NaOH solutions. It was found that the photodegradation of the aqueous dye solution could be enhanced by both H^+ and OH^- ion formation. Under acidic conditions, the perhydroxyl radical is formed by the protonation of superoxide radical. These perhydroxyl radicals combine together to form hydrogen peroxide, which in turn dissociates to give hydroxyl radical [Eqs (1)-(6)]. In the alkaline pH range the increased concentration of hydroxide ion results in the production of hydroxyl radicals [Eq. (7)].

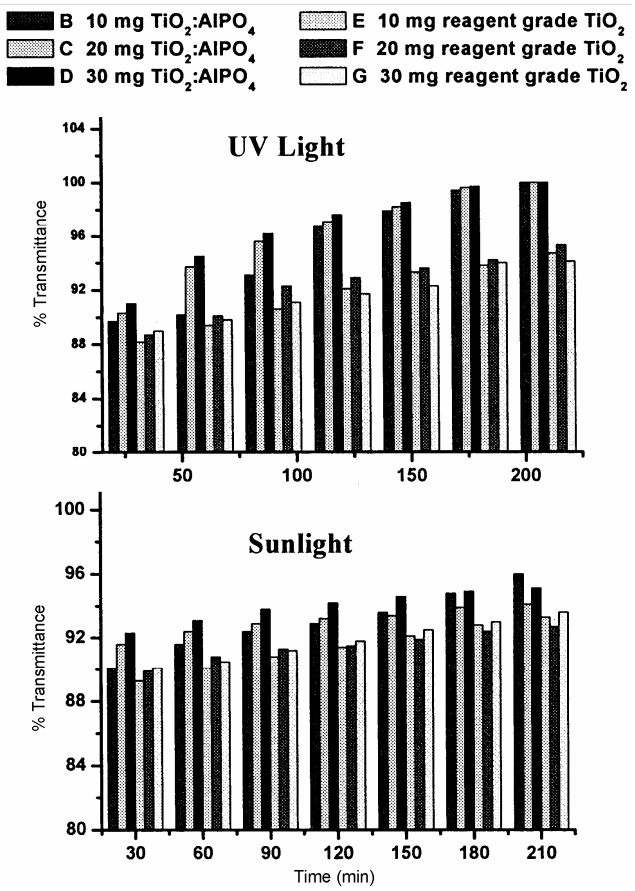

Fig. 5— Effect of TiO_2 : ($AlPO_4$-5) and TiO_2 on %T of indigo caramine dye under UV light, and sunlight

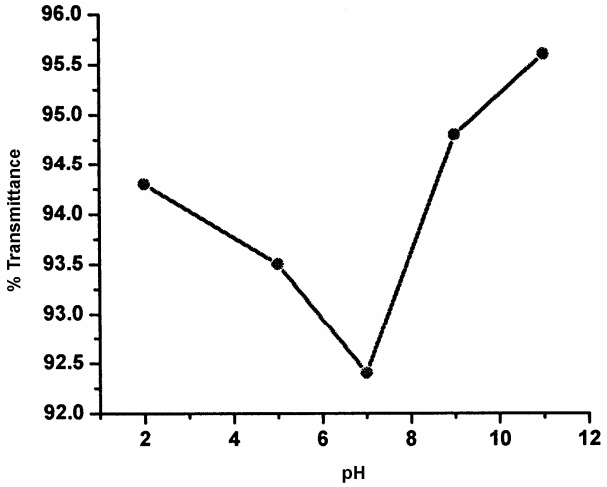

Fig. 6— Effect of pH versus percent transmission

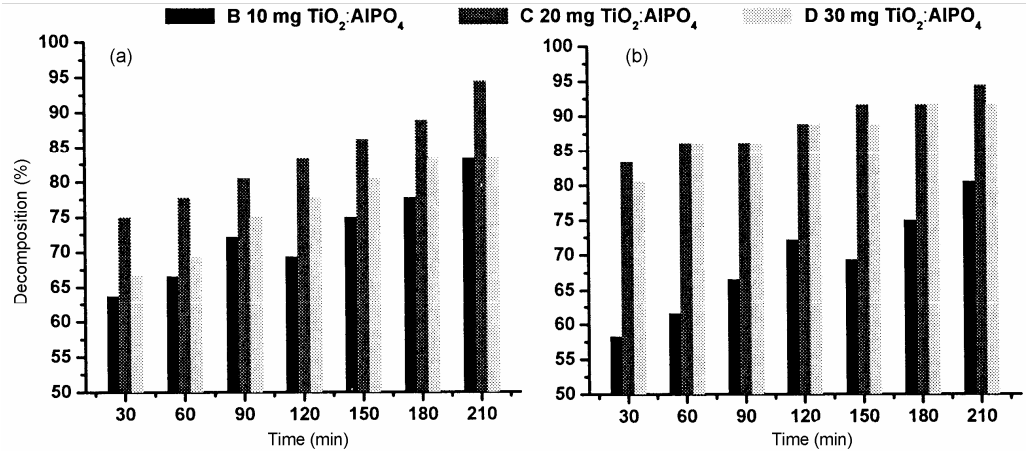

Fig. 7 — Degradation efficiency of TiO_2:($AlPO_4$-5) on indigo carmine dye: (a) UV light, (b) sunlight

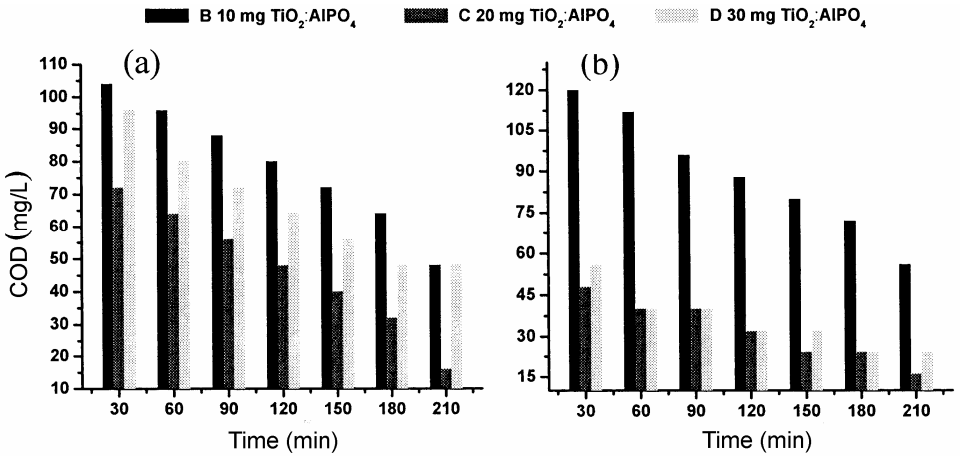

Fig. 8— Effect of TiO_2:($AlPO_4$ –5) on COD of the indigo carmine dye: (a) UV light, (b) sunlight

$$O_2 + e^- \xrightarrow{hv} \dot{O}_2^- \quad \ldots (1)$$

$$\dot{O}_2^- + H^+ \rightarrow H\dot{O}_2 \quad \ldots (2)$$

$$H\dot{O}_2 + H\dot{O}_2 \rightarrow H_2O_2 + O_2 \quad \ldots (3)$$

$$H_2O_2 + e^-_{CB} \xrightarrow{hv} H\dot{O} + HO^- \quad \ldots (4)$$

$$H_2O_2 + \dot{O}_2^- \rightarrow H\dot{O} + HO^- + O_2 \quad \ldots (5)$$

$$H_2O_2 \xrightarrow{hv} 2H\dot{O} \quad \ldots (6)$$

$$O_2 + HO^- \xrightarrow{hv} \dot{O}^- + H\dot{O} \quad \ldots (7)$$

Efficiency of TiO_2:$AlPO_4$-5 on the degradation of indigo carmine dye

In order to determine the optimal amount of the photocatalyst, a series of experiments were carried out with a varied amount of TiO_2:$AlPO_4$-5 composite. The dye concentration was maintained constant. It was found that the TiO_2:$AlPO_4$-5 shows high photocatalytic efficiency when compared to TiO_2 alone. Figure 7 illustrates the degradation efficiency of TiO_2:$AlPO_4$-5 composites on indigo carmine dye under UV and sunlight. The amount of the catalyst was varied between 10 and 30 mg in 50 mL of the aqueous dye solution. The degree of decolourization and decomposition of the dye solution increases with an increase in the amount of catalyst, and the highest efficiency was attained at 20 mg/50 mL. An increase in the decomposition efficiency is due to the increase in the number of active sites in TiO_2:$AlPO_4$-5 composites available for the reaction, which in turn increases the rate of radical formation.

The reduction in the decomposition efficiency may be due to the reduction in the penetration of light with surplus amount of TiO_2:$AlPO_4$-5. The excess addition of the catalyst makes the solution more turbid and the

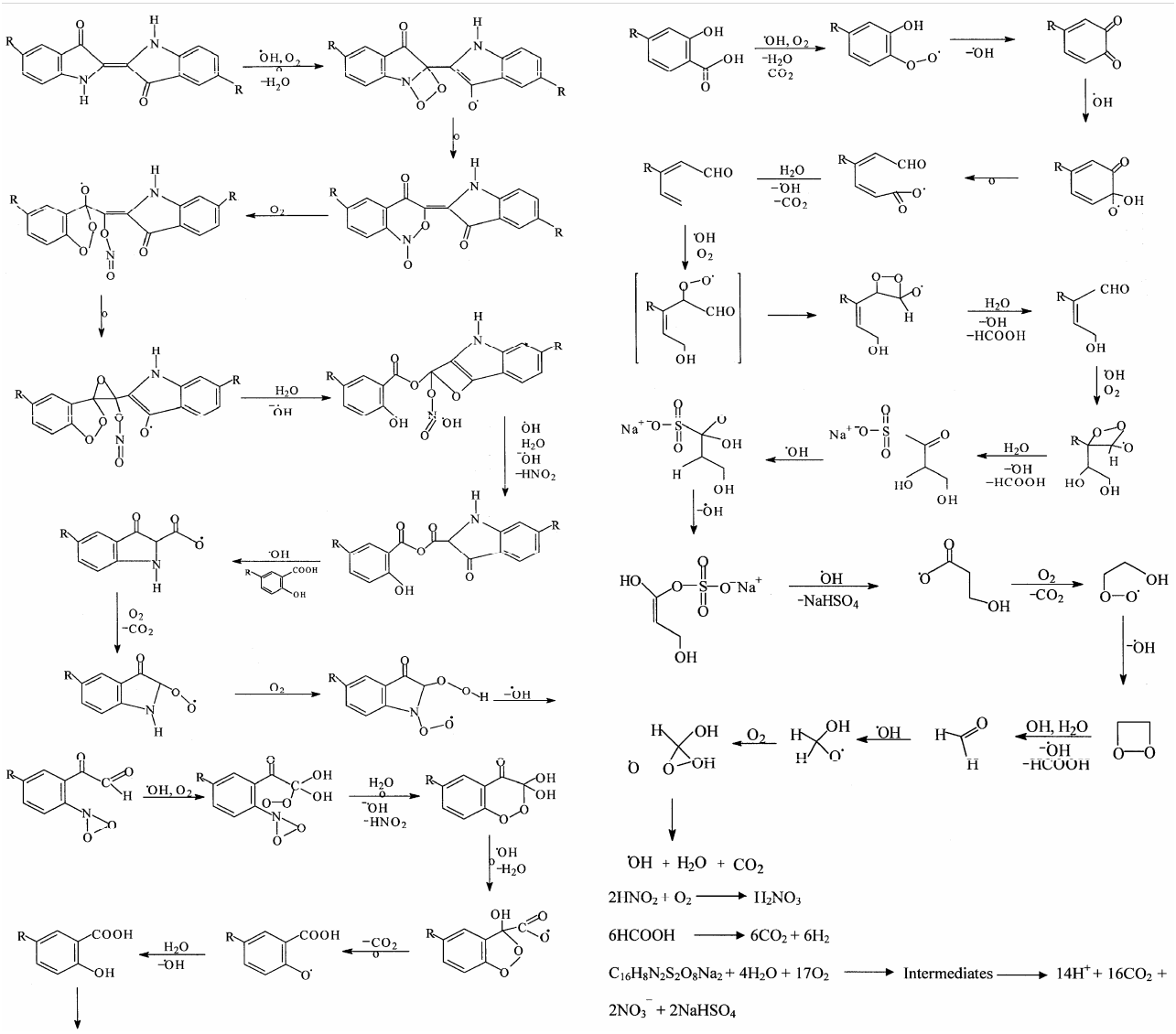

Fig. 9— Probable reaction mechanism for the photocatalytic degradation of Indigo carmine dye.

light reaching the catalyst surface is reduced. Further, the addition of surplus catalyst results in the deactivation of activated molecules by collision with ground state molecules and photodegradation efficiency decreases. Figure 8 shows the reduction in COD of the dye solution, which confirms the destruction of the organic molecules present in the dye solution. The comparative study was made on the rate of decomposition using TiO_2:$AlPO_4$-5 and TiO_2. It was observed that the result obtained on the decomposition rate of indigo caramine dye using TiO_2:$AlPO_4$-5 was higher when compared with that of the commercial TiO_2. The probable mechanism for the photodegradation of Indigo carmine dye is shown in Fig. 9.

Conclusion

TiO_2 coated or impregnated $AlPO_4$–5 zeolites are prepared under hydrothermal conditions for the photocatalytic degradation of indigo carmine dye. The XRD, FTIR and SEM studies resulted in the recognition of optimum conditions. The TiO_2:$AlPO_4$-5 zeolite composite was found to be very effective in the degradation of indigo carmine dye. The synergism between the TiO_2 catalyst and $AlPO_4$-5 zeolite is demonstrated. The decrease in COD value and the increase in %T and percentage decomposition

demonstrates the complete mineralization of the organics present in the dye solution. The comparative study of the photodegradation on %T and percentage decomposition of indigo caramine dye using

commercial TiO_2 and TiO_2:$AlPO_4$-5 has demonstrated the efficiency of the composite synthesised. The presence of the pores in the zeolite has helped in trapping the organics present in the dye solution thereby decolourising the dye solution and enhancing the penetration of light which is necessary for the photodegradation of the organics, on the other hand the TiO_2 present in the composite completely mineralized the organics trapped by the $AlPO_4$-5 as well as the organics present in the dye solution thereby making the TiO_2:$AlPO_4$- 5 composite as an efficient photocatalyst.

References

1 Pirkanniemi K & Sillanpaa M, *Chemosphere*, 48 (2002) 1047.

2 Deng X, Yue Y & Gao Z, *Appl Catal B*, 39 (2002) 135.

3 Chang C N, Ma Y S, Fang G C, Chao A C, Tsai M C & Sung H F, *Chemosphere*, 56 (2004) 1011.

4 Pichat P, Disdier J, Hoang-Van C, Mas D, Goutailler G & Gaysse C, *Catal Today*, 63 (2000) 363

5 Sang-Chul Jung, *Korean J Chem Eng,* 25(2) (2008) 364.

6 Liu X, Iu K K. & Thomas J K, *J Chem Soc, Faraday Trans,* 89 (1993) 1861.

7 Chen J, Eberlein L & Langford C H, *J Photochem Photobiol,* A 148 (2002) 183.

8 Corma A & Garcia H, *Chem Commun,* (2004) 1443.

9 Xu Y, Langford C H, *J Phys Chem,* 99 (1995) 11501.

10 Breck D W, *Zeolite Molecular Sieves* (Krieger: Malabar, Florida), 1984.

11 Dyer A, *An Introduction to Zeolite Molecular Sieves* (Wiley, New York), 1988.

12 Bekkum H V, Flanigen E M, Jacobs P A & Jansen J C, *Introduction to Zeolite Science and Practice*, 2nd edn (Elsevier, Amsterdam), 2001.

13 Matsuoka M & Anpo M, *J Photochem Photobiol, C* 3 (2003) 225.

14 Hashimoto S, *J Photochem Photobiol, C* 4 (2003) 19.

15 Peral J, Munoz J & *Domenech X, J Photochem Photobiol A: Chem*, (1989) 601.

16 Tayade Rajesh J, Kulkarni Ramchandra G & Jasra Raksh V, *Ind Eng Chem Res*, 46 (2007) 369.

17 Tayade Rajesh J, Surolia Praveen K, Lazar Manoj A & Jasra Raksh V, *Ind Eng Chem Res,* 47 (2008) 7545.

18 Lippincott E R, Van V A, Weir E E & Bunting E N, *J Res Natl Bur Std,* A61 (1958) 61.

19 Rao C N R., *Chemical Application of Infrared Spectroscopy* (Academic Press, New York), 1963.

20 Murov L S, *Handbook of Photochemistry* (Marcel Dekker, Inc., New York), 1973, 124.

21 Ferraz M C M, Maser E S & Jonhanuser M, *Fuel,* 78 (1999) 1567.

22 Lachheb H, Puzenat E, Houss A, Ksobi M, Elaloui E, Guillard C & Herrmann M, *Appl Catal B, Environ,* 39 (2002) 75.

23 Poulios I & Aetopoulon I, *Environ Technol,* 20 (1999) 479.

24 Reutergardh L B & Mallika I, *Chemosphere,* 35 (1997) 585.

25 Mills A & Hunte S L E, *J Photochem Photobiol A: Chem* (1977) 108.